

# The role of weak charging in metastable colloidal clusters

Christian L. Klix\*, Ken-ichiro Murata, and Hajime Tanaka†  
*Institute of Industrial Science, University of Tokyo, Meguro-ku, Tokyo 153-8505, Japan.*

Stephen R. Williams  
*Research School of Chemistry, The Australian National University, Canberra, ACT 0200, Australia.*

Alex Malins and C. Patrick Royall‡  
*School of Chemistry, University of Bristol, Bristol BS8 1TS, UK.*  
 (Dated: May 20th, 2009)

We study metastable clusters in a colloidal system with competing interactions. A short-ranged polymer-induced attraction drives clustering, while a weak, long-ranged electrostatic repulsion prevents extensive aggregation. We compare experimental yields of cluster structures expected from theory, which assumes simple addition of the competing isotropic interactions. For clusters of size  $4 \leq m \leq 6$ , the yield is significantly less than that expected. We attribute this to an anisotropic self-organized surface charge distribution linked to the cluster symmetry: non-additivity of electrostatic repulsion and polymer-induced attraction. 7-membered clusters have a clear optimal yield of the expected pentagonal bipyramid structure as a function of strength of the attractive interaction.

PACS numbers: 82.70.Dd; 82.70.Gg; 64.75.-g; 64.60.My

Clusters are intrinsically distinct from bulk matter, with the restricted degrees of freedom making their energy landscapes tractable, providing ideal model systems for studying kinetic pathways [1]. Although atomic clusters have been extensively studied, direct visualization is challenging and often limited to states of low temperature [2]. Colloidal dispersions provide a new medium by which to study clusters, and their well-defined thermodynamic temperature allows analogy with atomic, molecular, and protein clusters. Furthermore, the ability to track particle coordinates in 3D yields detailed static and dynamic information usually only accessible to computer simulation [3].

Colloidal dispersions feature novel cluster phases [4, 5, 6, 7], which open the possibility to synthesize colloidal clusters and ‘molecules’ [8, 9, 10, 11, 12] presenting exciting possibilities for new materials [13]. To fully realize the potential of colloidal clusters and ‘molecules’, it is necessary to understand their behavior, and in particular to investigate ways to optimize yields of desired structures [9]. Perhaps the simplest cluster-forming system is built around a spherically symmetric attraction which may be realized by adding non-adsorbing polymer to a colloidal suspension. The polymer osmotic pressure then leads to an effective attraction between the colloids known as the Asakura-Oosawa (AO) potential, whose strength is approximately proportional to the polymer concentration  $c_p$  [Fig. 1(a)].

While colloidal systems with purely attractive interactions may aggregate, stabilization can be achieved with longer-ranged electrostatic repulsions [5], which are often treated with a Yukawa (YUK) potential [14]. Here we combine the competing short-ranged attractions and weak long-ranged repulsions in colloidal systems with the well-understood behavior of clusters interacting via short-ranged attractions [15]. We neglect possible many-

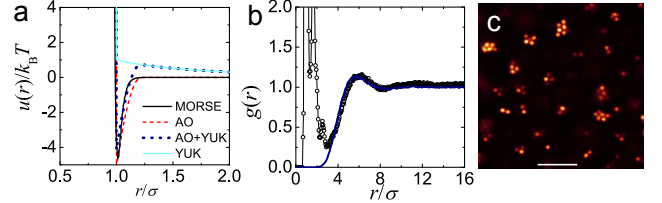


Figure 1: (color online) (a) Various potentials: Morse (black line) denotes a Morse potential for a well depth  $\epsilon_M = 4.6$  and  $\rho_0 = 33.1$ . AO (red dashed line) denotes Asakura-Oosawa for  $c_p = 6.02 \times 10^{-4}$ , YUK (light cyan line) denotes a Yukawa interaction for a contact potential of  $k_B T$  and inverse Debye screening length  $\kappa\sigma = 0.5$ . AO+YUK (blue dotted line) sums AO and YUK illustrating a treatment of the electrostatic repulsions as a small perturbation (see text). (b) Determining the repulsive interactions between the clusters. Experimental  $g(r)$  for  $c_p = 6.02 \times 10^{-4}$  (circles) and MC simulation (solid line) treating clusters as single particles, each with a charge  $Z = 61$ . (c) Confocal micrograph with  $c_p = 1.43 \times 10^{-3}$ . Bar is  $10 \mu\text{m}$ .

body interactions [16]. As Fig. 1(a) shows, for short interaction ranges the AO potential is similar to the Morse potential, whose range is set by a parameter  $\rho_0$ . Now the structures of the global energy minima for clusters of Morse particles are known [15], and for small clusters of size  $m < 8$ , the topology of this minimum structure is not sensitive to the range of the interaction, nor to weak, long-ranged Yukawa repulsions [18]. With the exception of  $m = 6$  (see below), the global minimum of small clusters in our colloidal system should therefore be identical to those tabulated for the Morse interaction [15]. Using a relatively dilute colloidal dispersion, we consider each cluster as a separate subsystem, and investigate the cluster structure at the single particle level. Using the

topological cluster classification algorithm [17], we compare the cluster structures found with those corresponding to Morse global energy minima, as a function of polymer concentration (strength of the attractive interaction) [15, 18]. As we shall see, even in our simple model system, the behavior is not as straightforward as one might expect. We believe this is due to a breakdown of the Yukawa description of the electrostatic interactions.

We used poly(methyl methacrylate) (PMMA) colloids sterically stabilized with polyhydroxyl steric acid. The colloids were labeled with fluorescent rhodamine dye and had a diameter of  $\sigma = 2.0 \mu\text{m}$  and a polydispersity of 4% as determined with static light scattering. The van der Waals interactions are neglected by closely matching the refractive index between the solvent and particles, sedimentation is avoided by matching the density. The colloid volume fraction was  $\phi \approx 0.02$ . We use a solvent composition of approximately 0.373 cis decalin, 0.093 cyclohexyl bromide and 0.533 tetrachloroethylene by mass, in which the dielectric constant  $\epsilon_R \approx 2.2$ . This is a good solvent for the polymer, polystyrene (PS). We used a molecular weight of  $3.0 \times 10^7$ , where our measurements of the interactions agreed well with the Asakura-Oosawa (AO) model with some swelling (35%) of the polymer [19], leading to a polymer-colloid size ratio  $q \approx 0.22$  which corresponds to a Morse potential with  $\rho_0 = 33.1$  [20]. We studied the system using confocal microscopy at the single particle level, using a Leica SP5, with which we track the particle coordinates to an accuracy of around 100 nm. We impose a bond length of  $1.4\sigma$ , this slightly larger value than the range of the attractive interaction reflects particle tracking errors and polydispersity. Our results are robust to reasonable changes in the bond length. We sampled typically  $10^5$  coordinates per state point. No change in the cluster populations was observed on the timescale of the experiments (1 day).

We find the order of magnitude of the colloid charge in cluster fluid by treating the clusters as individual particles and neglecting their different sizes [21]. The size distribution is shown in Fig. 2(a) for a polymer weight fraction  $c_p = 6.02 \times 10^{-4}$  the mean  $\langle m \rangle = 3.3$  and standard deviation is 4.4. In Fig. 1(b), we fit the radial distribution function  $g(r)$  with Monte Carlo simulation according to a Yukawa potential [14], yielding  $Z = 61 \pm 20$  charges per cluster, and a Debye screening length of  $\kappa^{-1} = 2.0 \pm 0.4\sigma$ . This suggests around 10–20 charges per colloid, which corresponds to a Yukawa potential at contact of  $\beta\epsilon_{\text{YUK}} = Z^2 l_B / [(1 + \kappa\sigma/2)^2 \sigma] \sim 1-3$  where  $\beta = 1/k_B T$  ( $k_B$ : Boltzmann's constant)  $l_B \approx 25$  nm is the Bjerrum length. Although this charge is very low, similar values have been measured for PMMA in apolar solvents [22]. A confocal microscopy image of the system is shown in Fig. 1(c), we see the clusters are well isolated, consistent with our assumption that each cluster may be treated as a separate system. Increasing  $c_p$  promotes clustering.

We now proceed to consider the behavior of the individual clusters (as a separate system). Figure 2(b) shows

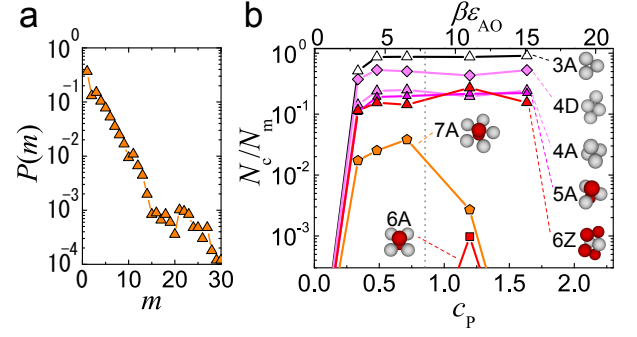


Figure 2: (color online) (a) Cluster size distribution for  $c_p = 6.02 \times 10^{-4}$ . (b) ‘Structural yield’  $N_c/N_m$  as a function of  $c_p$ . Only in the case of  $m = 3$  does the yield of the global energy minimum (3A) approach 100%. Vertical dashed line denotes polymer overlap.  $\beta\epsilon_{\text{AO}}$  is the contact potential for the AO interaction.

the ‘structural yield’  $N_c/N_m$  as a function of the attractive interaction  $c_p$ .  $N_c$  is the number of clusters of a given structure,  $N_m$  is the total number of clusters containing  $m$  colloids. For the smaller cluster sizes a greater portion are found in the Morse global minimum, with the exception of the octahedral 6A cluster which is much less popular than either the triangular bipyramid 5A or the pentagonal bipyramid 7A. Considering the topology of the 3A, 4A, 5A, and 6A clusters we see that the distance between all the nearest neighbors will be the same due to the short range nature of the AO potential and next nearest neighbors do not contribute, if we ignore the weak electrostatic repulsion. The minimum energy for these clusters is thus approximately proportional to the number of nearest neighbors or contacts. However, for  $m = 6$ , global minimum for the Dzugutov potential [23] has a  $C_{2v}$  point group symmetry and the same number of contacts as 6A. We therefore seek the this 6Z cluster using the TCC.

Neglecting the weak charge, both 6A and 6Z clusters have the same ground state potential energy but there are other contributions to the cluster’s free energy: configurational entropy and electrostatic energy. Indistinguishability arguments suggest that 6Z should be 12 times as popular as 6A. Moreover, 6Z is further favored by its larger radius of gyration, which lowers electrostatic energy [24]. As we shall see below, the effects even of these weak electrostatic interactions can be rather complex. However, the very large population difference in this system is suggestive of a further mechanism at play: the kinetic pathway and the associated energy barrier. Addition of particles leads to the sequence  $3A \rightarrow 4A \rightarrow 5A \rightarrow 6Z$  while the formation of 6A requires a bond to be broken and insertion of a particle to form the 4-membered square ring.

We expect an increase of polymer concentration (lowering of the effective temperature) to promote clusters which maximize the number of bonds, *i.e.* 3-7A, or 6Z. This we see in Fig. 2(b) for  $m = 3$ , in the near 100%

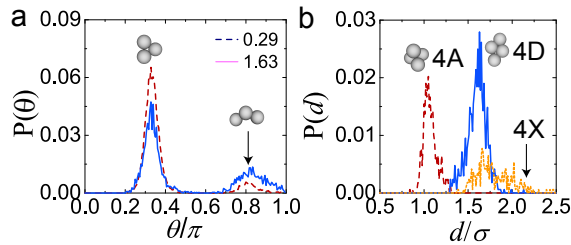


Figure 3: (color online) (a) Distribution of bond angles  $\theta$  for  $m = 3$  clusters. As  $c_p$  (listed  $\times 10^{-3}$ ) is increased, the population of 3A triangles increases. (b) Maximum center separation,  $m = 4$ . Red dashed line denotes 4A tetrahedron, blue (solid) line 4D diamond and orange (dotted) line ('4X') higher energy (fewer bonds).  $c_p = 7.1 \times 10^{-4}$ .

yield of 3A triangles at high  $c_p$ . In Fig. 3 (a) we show the distribution of bond angles  $\theta$  in  $m = 3$  at different polymer concentrations. In addition to a higher 3A triangle population at higher  $c_p$ , we see a peak at large bond angle, showing that an elongated structure is preferred, and that the system seems to sit either in a triangle or the linear structure. We attribute this two-state behavior to the fact that the colloids carry a (weak) charge, promoting elongated states [24]. In the case of more complex clusters, such as 7A, an initial increase in yield with  $c_p$  is followed by a decrease, presumably due to frustration, at high interaction strength.

However, intermediate cluster sizes,  $4 \leq m \leq 6$  show a surprising behavior, with little sensitivity to polymer concentration. Motivated by our analysis of  $m = 3$  clusters, we consider structures in addition to the ground state 4A tetrahedron in the  $m = 4$  population. Here we consider the largest separation of colloid centers  $d$ . Now  $d \approx \sigma$  for 4A tetrahedra, while the maximum value is  $d \approx 3\sigma$  for a line of 4 particles. Figure 3(b) shows two dominant structures in the  $m = 4$  population: the 4A tetrahedra and a diamond-shaped structure we term 4D, which is distinct from a square structure for which  $d = \sqrt{2}\sigma$ . Unlike more complex (e.g. 7A) clusters, for  $m = 4$ , there is no geometric frustration in the formation of tetrahedra. In fact Brownian dynamics simulations of four particles interacting via the Morse potential [25] show a clear peak in the 4D population, and a tendency to form tetrahedra at strong interaction strength [Fig. 4(a)]. Furthermore, using an *isotropic* Yukawa interaction with parameters similar to those found in our experiments has little effect: we see a high yield of 4A at large  $\beta\epsilon_M$ , consistent with [18].

Why then do the experiments have such a high 4D population? One argument might be that the AO model is starting to break down as we exceed overlap, which occurs at  $c_p \approx 8.5 \times 10^{-4}$  as indicated in Fig. 2. However for this size ratio we expect only a slight effect in the AO interactions at overlap [26]. Instead, we postulate that 4D is stabilized by the weak charging present in this system, which unlike the spherically symmetric distribution often assumed, may be anisotropically distributed

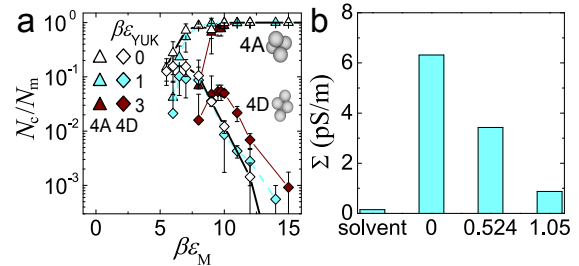


Figure 4: (color online) (a) Structural yields  $N_c/N_m$  as a function of well depth  $\beta\epsilon_M$  calculated from Brownian dynamics simulations for the Morse potential for  $\rho_0 = 33.1$  for  $m = 4$ . Diamonds denote 4D and triangles 4A. Thick lines with unfilled symbols denote Yukawa contact potential  $\beta\epsilon_{YUK} = 0$ , light blue (dashed)  $\beta\epsilon_{YUK} = 1$  and thin crimson lines and filled symbols  $\beta\epsilon_{YUK} = 3$  and inverse Debye screening length  $\kappa\sigma = 0.5$ . (b) Conductivity of the solvent, and colloidal suspension at various polymer concentrations  $\times 10^{-3}$ .

on colloid surfaces, leading to anisotropic electrostatic interactions [7].

While electrostatic charging mechanisms in these non-aqueous systems are not yet fully understood, it is reasonable to suppose that charging may be related to the free colloid surface, which may be reduced upon clustering. To this end, we measured the conductivity of the system as a function of  $c_p$  with dielectric spectroscopy [Fig. 4(b)]. As we do not add salt, we assume the system is in the counter-ion dominated regime, and we note a large increase in conductivity relative to the pure solvent. What is evident from Fig. 4(b) is that the introduction of the colloids massively increases the conductivity relative to the pure solvent, and that adding polymer then decreases the conductivity. We associate this reduction in ionic strength (charge per colloid) with clustering, and argue that the charge is indeed associated with the free surface of the colloids, which is reduced upon clustering. While precise determination of the ionic strength from conductivity measurements requires detailed knowledge of the ionic species present, assuming Walden's rule and a typical limiting molar conductance for ions in these systems of  $4 \text{ cm}^2 \text{ mol}^{-1}$  [14] we arrive at an ionic strength around  $10^{-10} \text{ M}$ , consistent with the Debye length  $\kappa^{-1} \sim 2\sigma$  found with our MC simulations [Fig. 1(b)].

4D and 4A clusters are formed by an attachment of one particle to 3A. For  $3A \rightarrow 4A$  there are three direct contact points to be formed, whereas for  $3A \rightarrow 4D$  there are only two. Thus 4D may be more easily formed than 4A due to a reduced electrostatic barrier and smaller loss of translational entropy of counter ions. We note that the latter factor is not considered at all in a model with a Yukawa potential. Furthermore, we stress that a Yukawa potential should break down at short distances and thus fail in describing aggregation of particles. For 4D  $d \sim \sqrt{3}\sigma$  whereas for 4A  $d \sim \sigma$ . So 4D is more favored than 4A electrostatically. We note that although there is no struc-

tural frustration in the 4D→4A transition, there is only one path, if no bonds are broken; one or both of the two end particles must ‘roll’ around the central two. We note that the 4D-4A transformation, always leads to a decrease in  $d$ , which may be prohibited by electrostatic repulsions. Thus, once 4D is formed, the transformation from 4D to 4A is suppressed: kinetic arrest. That 4D formation is promoted and 4D→4A transformation is suppressed due may lead to the high fraction of 4D. It is possible that the charging mechanism leads to a scenario in which the equilibrium populations are a distribution dominated by both 4D and 4A as found. However, the lack of response of the system to increasing the strength of attraction by a factor of three leads us to the conclusion that some form of kinetic arrest is more likely. On the other hand, our results suggest that it is not so difficult to make a 3A triangle from a linear cluster. Although the reason for the difference is not immediately clear, we note that the linear→3A transition is not geometrically constrained to follow a single path.

Here we consider some microscopic aspects of this problem. The low surface charge density (small  $Z$ ) implies that the discrete nature of charges may be important. Furthermore, the recombination rates of ions might be very slow: even for small ions, diffusion-controlled reaction rate constants are  $10^9$ - $10^{10}$   $\text{dm}^3\text{M}^{-1}\text{s}^{-1}$ , of order seconds or tens of seconds here. For the larger ions or

complexes relevant to these apolar solvents [14, 22] the rate may be lower still. That the charges are discrete in both space and time may play an important role in the above-described frustration. Further work is necessary for elucidating the exact mechanism responsible for the observed cluster type distribution.

Our study suggests that the one-component description is breaking down, even for these simple colloidal systems. In the case of  $m = 6$ , two structures with similar energies compete, however, the 6Z is very much more popular than the 6A octahedron. Although equilibrium arguments favor this trend we note that 6Z is structurally similar to 5A, and thus may likely be kinetically favored. The yield of the fivefold symmetric 7A shows signs of frustration at relatively deep quenches, reminiscent of patchy particles [9]. Our results form the beginnings of an understanding of self-assembly of colloidal molecules as a function of attraction strength; we hope they will stimulate the development of more powerful models.

The authors are grateful to Wuge Briscoe, Didi Derks, Jeroen van Duijneveldt, Rob Jack and Matthias Schmidt for a critical reading of the manuscript. CLK thanks the Deutscher Akademischer Austauschdienst for financial assistance. CPR acknowledges the Royal Society for financial support. HT acknowledges a Grant-in-Aid from the Ministry of Education, Culture, Sports, Science and Technology, Japan.

- 
- [\*] \* Present address: University of Konstanz, 78457 Konstanz, Germany.
- [†] †E-mail: tanaka@iis.u-tokyo.ac.jp
- [‡] ‡E-mail: paddy.royall@bristol.ac.uk
- [1] D. J. Wales, *Energy Landscapes: Applications to Clusters, Biomolecules and Glasses* (Cambridge University Press, Cambridge, Cambridge, 2004).
  - [2] Z. Li, N. Young, M. Di Vece, S. Palomba, R. Palmer, A. Bleloch, B. Curley, R. Johnston, J. Jiang, and J. Yuan, *Nature* **451**, 46 (2008).
  - [3] A. van Blaaderen and P. Wiltzius, *Science* **270**, 1177 (1995).
  - [4] P. N. Segre, V. Prasad, A. B. Schofield, and D. A. Weitz, *Phys. Rev. Lett.* **86**, 6042 (2001).
  - [5] A. Stradner, H. Sedgwick, F. Cardinaux, W.-C. Poon, S. Egelhaaf, and P. Schurtenberger, *Nature* **432**, 492 (2004).
  - [6] A. I. Campbell, V. J. Anderson, J. S. van Duijneveldt, and P. Bartlett, *Phys. Rev. Lett.* **94**, 208301 (2005).
  - [7] L. Hong, A. Cacciuto, E. Luijten, and S. Granick, *NanoLett.* **6**, 2510 (2006).
  - [8] V. N. Manoharan, M. T. Elsesser, and D. J. Pine, *Science* **301**, 483 (2003).
  - [9] A. W. Wilber, J. P. K. Doye, A. A. Louis, E. G. Noya, M. A. Miller, and P. Wong, *J. Chem. Phys.* **127**, 085106 (2007).
  - [10] E. G. Noya, C. Vega, J. P. K. Doye, and A. A. Louis, *J. Phys. Chem.* **127**, 054501 (2007).
  - [11] S. M. Anthony, M. Kim, and S. Granick, *J. Chem. Phys.* **129**, 244701 (2008).
  - [12] D. Zerrouki, J. Baudry, D. Pine, P. Chiakin, and J. Biette, *Nature* **455**, 380 (2008).
  - [13] S. C. Glotzer and M. J. Solomon, *Nature Materials* **6**, 557 (2007).
  - [14] C. Royall, M. Leunissen, A.-P. Hynninen, M. Dijkstra, and A. van Blaaderen, *J. Chem. Phys.* **124**, 244706 (2006).
  - [15] J. P. K. Doye, D. J. Wales, and R. S. Berry, *J. Chem. Phys.* **103**, 4234 (1995).
  - [16] H. Löwen and E. Allahyarov, *J. Phys.: Condens. Matter* **10**, 4147 (1998).
  - [17] C. P. Royall, S. R. Williams, T. Ohtsuka, and H. Tanaka, *Nature Mater.* **7**, 556 (2008).
  - [18] S. Mossa, F. Sciortino, P. Tartaglia, and E. Zaccarelli, *Langmuir* **20**, 10756 (2004).
  - [19] C. P. Royall, A. Louis, and H. Tanaka, *J. Chem. Phys.* **127**, 044507 (2007).
  - [20] M. G. Noro and D. Frenkel, *J. Chem. Phys.* **113**, 2941 (2000).
  - [21] F. Sciortino, S. Mossa, E. Zaccarelli, and P. Tartaglia, *Phys. Rev. Lett.* **93**, 055701 (2004).
  - [22] G. Roberts, T. Wood, W. Frith, and P. Bartlett, *J. Chem. Phys.* **126**, 194503 (2007).
  - [23] J. P. K. Doye, D. J. Wales, and S. I. Simdyankin, *Faraday Discuss.* **118**, 159 (2001).
  - [24] J. Groenewold and W. Kegel, *J. Phys. Chem. B* **105**, 11702 (2001).
  - [25] A. Malins, S. Williams, J. Eggers, H. Tanaka, and C. P. Royall, submitted (2009).
  - [26] A. A. Louis, P. G. Bolhuis, E. J. Meijer, and J. P. Hansen,

J. Chem. Phys. **117**, 1893 (2002).